The International Journal of Advanced Manufacturing Technology (2018) 98:1355–1365
https://doi.org/10.1007/s00170-018-2317-y

ORIGINAL ARTICLE

Effect of cutting parameters on surface quality in multi-step turning of Ti-6Al-4V titanium alloy

Guanming Hou[1] · Anhai Li[1,2] · Xuhao Song[1] · Hu Sun[1] · Jun Zhao[1,2]

Received: 1 March 2018 / Accepted: 5 June 2018 / Published online: 19 June 2018

Abstract
In the multi-step cutting process, the final machined surface quality is affected by the entire cutting process, especially the effect of work hardening and thermal softening induced by the previous steps (roughing or semi-finishing machining). In this paper, two-step (roughing-finishing) and three-step (roughing-semi-finishing-finishing) turning operations were designed by a single-factor experiment, and the effect of the change of cutting parameters in the previous steps on finishing surface quality was analyzed. Experimental results indicated that the microhardness in the machined surface layer of semi-finishing was smaller than that of roughing at the same depth, and the depth affected by work hardening of semi-finishing was thinner. Therefore, compared to two-step machining, the surface roughness affected by the work hardening and thermal softening of the previous steps was smaller after three-step machining, and the variation range of surface roughness with the change of the cutting parameters was smaller. Moreover, the relative height between the convex peak and the concave valley was larger. And the spacing between adjacent two convex peaks became larger and more uneven after three-step machining. The disturbed layer depth or the plastic deformation layer (PDL) depth was obviously reduced. However, the grains were severely distorted and stretched. It was because that semi-finishing weakened the work hardening of roughing in the three-step cutting process; therefore, the surface quality was better after finishing. By studying the effect of work hardening and thermal softening induced by the previous steps on finishing surface quality, the cutting parameters of roughing and semi-finishing were optimized to ultimately improve surface quality.

Keywords Multi-step turning · Work hardening · Surface topography · Microstructure · Titanium alloy

1 Introduction

With the rapid development of modern technology, especially in the field of high-end equipment manufacturing such as aerospace and marine navigation, the requirements on the surface quality of high-speed machining are getting higher and higher. Titanium alloy Ti-6Al-4V is widely used due to their excellent mechanical properties. However, the inherent properties such as low thermal conductivity and low modulus of elasticity of titanium alloy cause great difficulties for high-speed machining [1]. The machined surface defects or bad surface integrity is the main part that leads to early failure of material corrosion, friction, and fatigue, so to optimize and improve the surface quality are the key to improving the material service life. However, surface quality is affected by many factors [2–4], especially cutting parameters and tool parameters as well as tool flank wear [5–12]. The effect of the cutting parameters on the surface quality during the cutting process is very complicated, and it is a multi-factor comprehensively interacting process, which involves the cutting force, cutting temperature, the extrusion, and friction between the tool and the machined surface. The differences of cutting force and cutting temperature will have an effect on the surface roughness, microhardness, residual stress, the disturbed layer or PDL, and so on, and ultimately affect the material service life.

Different degrees of material pretreatment can also affect the surface quality, such as heat treatment and rolling. The AISI 4340 steel was heat-treated under different conditions to change the microhardness of surface layer. It was found

✉ Anhai Li
anhaili@sdu.edu.cn

[1] Key Laboratory of High Efficiency and Clean Mechanical Manufacture of MOE, School of Mechanical Engineering, Shandong University, Jinan 250061, People's Republic of China

[2] National Demonstration Center for Experimental Mechanical Engineering Education (Shandong University), Jinan 250061, People's Republic of China

that the surface residual stress changed from tensile stress to compressive stress in the cutting process. As the microhardness increased, it changed the distance from the peak of residual compressive stress to surface [13].

Currently, the researches on surface quality are mostly focused on the single-step machining process (roughing or finishing). However, in the actual machining process, the products are usually obtained through multi-step cutting. Because of the influence of cutting force, cutting temperature, and strain accumulation [14, 15], compared to the bulk material, the mechanical properties of machined surface layer were significantly modified, which further affected the later machining process. For milling hardened steel SKD11, the experiment and simulation found that, compared to the first step machining, the extrusion and friction between the tool and the machined surface were more intense when the second step was machined, which led to a significant increase in the residual compressive stress [16]. The results of multi-step cutting simulation on an annealed 304 stainless steel [17] showed that the machined surface layer affected by the first step had an effect on the chip thickness, cutting forces, residual strain, and cutting temperature. At the same time, the distribution and depth of the residual stress were significantly changed. According to simulation results, characteristics of residual stress could be controlled by optimizing the second cut. However, when the Cu-Zn alloy was studied through experiments and simulations, it was found that the residual tensile stress appeared on the surface after roughing or finishing [18]. On the contrary, residual compressive stress appeared on the surface after roughing and finishing. Mainly because the strain and stress were remained in certain depth of the machined surface layer, and the layer had the distribution of microhardness caused by work hardening. But the surface was residual tensile stress after roughing and then two or three times finishing.

It was found that the machined surface layer depth affected by roughing was more than 0.3 mm in the high-speed machining process of titanium alloy [19, 20]. The machined surface layer affected by cutting force and cutting temperature was severely work-hardened and softened at different depths after roughing, which would seriously affect the finishing cutting process and ultimately affect the surface quality.

Multi-step cutting is a multi-step loading and stress relaxation process, and the final surface quality depends on the entire cutting process. In particular, strain accumulation and temperature induced by the previous steps lead to a big difference between the machined surface layer and bulk material in terms of microhardness and residual stress. Therefore, the mechanical properties of machined surface layer and subsurface layer were altered before the finishing operation [19, 21]. In this paper, a multi-step turning process was conducted by single-factor cutting experiments. Vickers microhardness was measured along the machined surface layer after the roughing and semi-finishing, respectively. At the same time, the effect of work hardening and thermal softening induced by the previous steps on finishing surface quality were studied, especially from the following aspects of the surface roughness, surface topography, and microstructure. And the effect of the variation of cutting parameters of the previous steps on finishing machining was revealed. Eventually, the parameters of multi-step machining were further optimized to improve the surface quality.

2 Cutting materials and experimental conditions

The workpiece material used in the experiment was titanium alloy Ti-6Al-4V, and the chemical compositions of the material and mechanical properties were given in Tables 1 and 2, respectively. And microstructure and phase compositions of titanium alloy Ti-6Al-4V were shown in Fig. 1. The samples used in the machining process were titanium alloy bars with the diameter 100 mm and the length 25 mm. A multi-step cutting diagram was shown in Fig. 2.

All turning experiments were carried out on a CKD6150K turning lathe under dry cutting conditions. The coated carbide tools were used, the type of roughing tools was SNMG120408-EF, and the type of semi-finishing and finishing tools was SNMG120404-EM. The tool angle after installed was 14° of rake angle and 11° of clearance angle when machining. The final surface quality was obtained through two-step machining (firstly roughing and finally finishing) and three-step machining (firstly roughing, then semi-finishing, and finally finishing). In the two-step machining process, the roughing cutting parameters were variable, as shown in Table 3. However, finishing cutting parameters were constants, and the cutting process was carried out at the cutting speed of 100 m/min, feed rate of 0.05 mm/r, and depth of cut of 0.1 mm. In the three-step machining process, the roughing cutting parameters were fixed values, and the cutting process was carried out at the cutting speed of 50 m/min, feed rate of 0.25 mm/r, and depth of cut of 1 mm. And the semi-finishing parameters were variable, as shown in Table 4. Consistent with the two-step machining, the same finishing parameters were used. At the same time, in order to reduce the impact of the tool on the cutting process, new tools were used for each cutting operation.

The surface roughness of each sample after finishing was measured by a hand-held surface roughness meter. Each

Table 1 Chemical composition of titanium alloy Ti-6Al-4V

Elements	Al	V	Fe	C	N	H	O	Other	Ti
Weight (wt%)	5.5–6.75	3.6–4.5	0.3	0.08	0.05	0.15	0.10	0.50	Base

Table 2 Mechanical and physical properties of titanium alloy at room temperature

Density (kg/m^3)	Melting point (°C)	Specific heat (25 °C) (J/kg·°C)	Thermal conductivity (W/m·K)	Yield stress (MPa)	Young's modulus (GPa)	Poisson's ratio	Elongation (%)
4428	1605	580	7.3	825	110	0.41	10

sample was measured seven times to acquire accurate results along the circumferential direction in different areas and then the average of the seven measured values was taken as the surface roughness value. Three-dimensional (3D) machined surface topography after finishing was measured by using 3D-zoom surface measurement instrument (VK-X250K), and the area of sampling point is 467 mm × 624 mm. The HVS-1000 microhardness instrument was used to measure the microhardness of the machined surface layer after roughing or semi-finishing, at a load of 100 g and waiting time of 15 s. Considering the indenter, the measurement of microhardness was started at the depth of 20 μm below the machined surface and every 10-μm interval, was measured until the measured microhardness value was close to the bulk microhardness of the material; the measurement diagram was illustrated in Fig. 3. And the same depth was measured three times during the measurement to reduce the error. Using the cross-sectional method, the microstructure of the finishing machined surface layer was observed by using a scanning electron microscope (SEM) and a VHX-600 ESO digital microscope. For the convenience of measurement, the sample was cut by wire electrical discharge machining, cut into small pieces along the cutting machining direction for inlaying, ground using sandpaper, and then polished with diamond grits until the surface to be measured appeared mirror. The cross-sections of samples were chemically etched by corrosive liquid that was made up of HNO_3, HF, and H_2O, according to the ratio of 5:3:100. Each sample was etched for 25 s and cleaned for final observation. At the same time, in order to obtain the desired microstructure, each sample is magnified 2000 times.

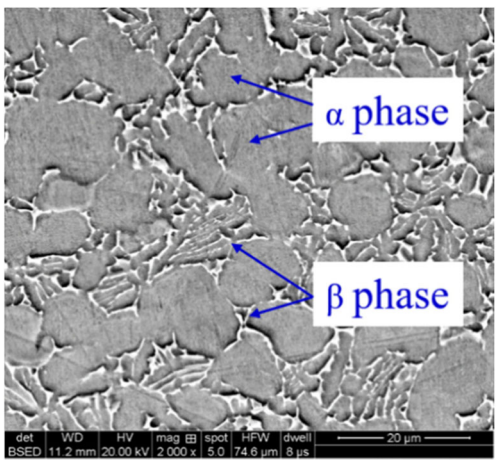

Fig. 1 The microstructure and phase compositions of titanium alloy Ti-6Al-4V

3 Results and discussion

In this experiment, the influences of the change of roughing cutting parameters in the two-step machining process and semi-finishing cutting parameters in the three-step machining process were studied, respectively, in terms of the microhardness, surface roughness, and surface topography, as well as subsurface microstructure. The microhardness of machined surface layer was measured after roughing or semi-finishing. When analyzing the results of surface roughness, surface topography, and surface microstructure, since the finishing cutting parameters were constants, the horizontal axis was the roughing or semi-finishing cutting parameters, while the vertical axis was the finishing measurement results.

3.1 Microhardness

In the high-speed machining process of titanium alloy Ti-6Al-4V, the change of cutting parameters and tool parameters will affect cutting force, cutting temperature, extrusion, friction, etc. However, due to the poor thermal conductivity of titanium alloy, the accumulation of temperature in the contact area between the tool and the workpiece results in the softened layer generated near the machined surface layer. At the same time,

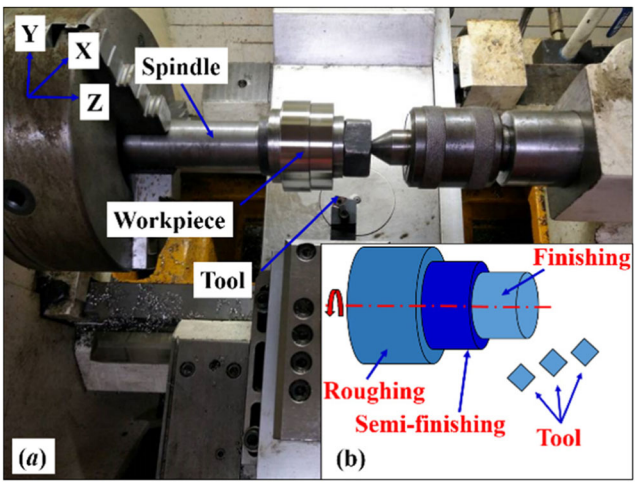

Fig. 2 Cutting experiment. (a) Experiment equipment and (b) cutting diagram

Table 3 Roughing cutting parameters of two-step machining

Level	Cutting speed v (m/min)	Feed f (mm/r)	Depth of cut a_p (mm)
1	30	0.25	1.00
2	40	0.25	1.00
3	50	0.25	1.00
4	60	0.25	1.00
5	70	0.25	1.00
6	50	0.15	1.00
7	50	0.20	1.00
8	50	0.30	1.00
9	50	0.35	1.00
10	50	0.25	0.50
11	50	0.25	0.75
12	50	0.25	1.25
13	50	0.25	1.50

because of cutting force, hardened layer is generated beneath the softened layer with the increase of depth. Finally, due to lack of the effect of cutting force, it will be bulk material beneath the hardened layer. Therefore, it could be divided into three different zones including the softened zone, the hardened zone, and the bulk material zone beneath the machined surface [22].

According to the analysis of the measured microhardness value for all samples, the microhardness beneath the machined surface is shown in Figs. 4 and 5. Figure 4 showed the distribution of microhardness, with the change of cutting speed, feed, and depth of cut, respectively, which was measured along the machined surface layer after roughing. At the same time, Fig. 5 was respectively the distribution of microhardness after semi-finishing with the change of feed or depth of cut. It could be seen from Figs. 4 and 5 that, with the change of cutting speed, feed, and depth of cut, the distribution of microhardness along machined surface layer was generally consistent; microhardness value increased firstly along machined surface layer and then decreased, and finally close to the bulk microhardness (BMH) value.

Table 4 Semi-finishing cutting parameters of three-step machining

Level	Cutting speed v (m/min)	Feed f (mm/r)	Depth of cut a_p (mm)
1	80	0.05	0.3
2	80	0.10	0.3
3	80	0.15	0.3
4	80	0.20	0.3
5	80	0.25	0.3
6	80	0.15	0.1
7	80	0.15	0.2
8	80	0.15	0.4
9	80	0.15	0.5

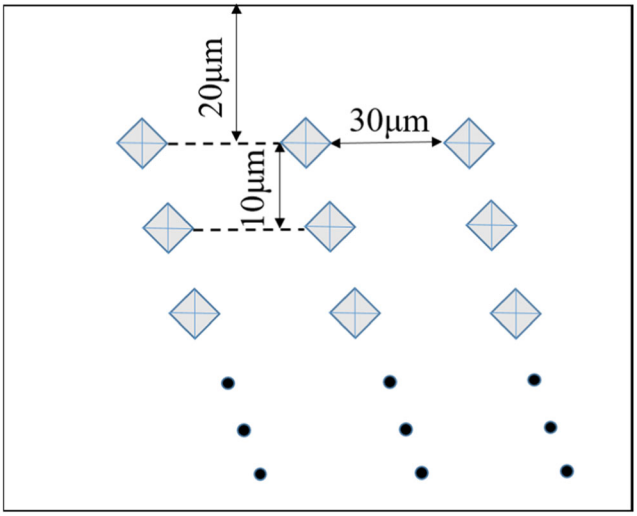

Fig. 3 The diagram of microhardness measurement

It could be found from Fig. 4a that, with the increase of cutting speed within the experimental range, the microhardness value had a declining trend at 20 μm, the maximum microhardness increased beneath the machined surface, and the depth of hardening increased obviously. It could be seen from Fig. 4b, compared to cutting speed, the change of feed did not affect obviously the microhardness of machined surface layer. From Fig. 4c, it could be seen that, with the increase of the depth of cut, the maximum value of microhardness increased obviously in machined surface layer. The distance of the maximum microhardness to the machined surface increased and the depth of the machined surface layer affected by cutting process increased obviously. It was shown from Fig. 5a, b that, compared to Fig. 4a–c, the microhardness value of the machined surface layer decreased obviously at 20 μm after semi-finishing, the maximum microhardness value decreased relatively, and the distance of the maximum microhardness to the machined surface decreased and the depth of the machined surface layer decreased obviously. Compared to the effect of roughing cutting parameters on the microhardness of machined surface layer, the effect of semi-finishing was relatively reduced.

From Fig. 4a or b or c, it could be seen that, when machining at the cutting speed of 50 m/min, feed of 0.25 mm/r, and depth of cut of 1 mm, the maximum microhardness of machined surface layer was about 100 μm beneath the surface, and the depth of the machined surface layer affected by cutting process exceeded 160 μm. It could be seen from Fig. 5a that it is the same as the change of feed parameters in the roughing cutting process, the change of semi-finishing has little effect on the microhardness of machined surface layer, but the microhardness is significantly lower than the microhardness of roughing at same depth. It could be seen from Fig. 5b that although there were two cutting processes at the depth of cut of 0.1 and 0.2 mm, the distributions of microhardness along

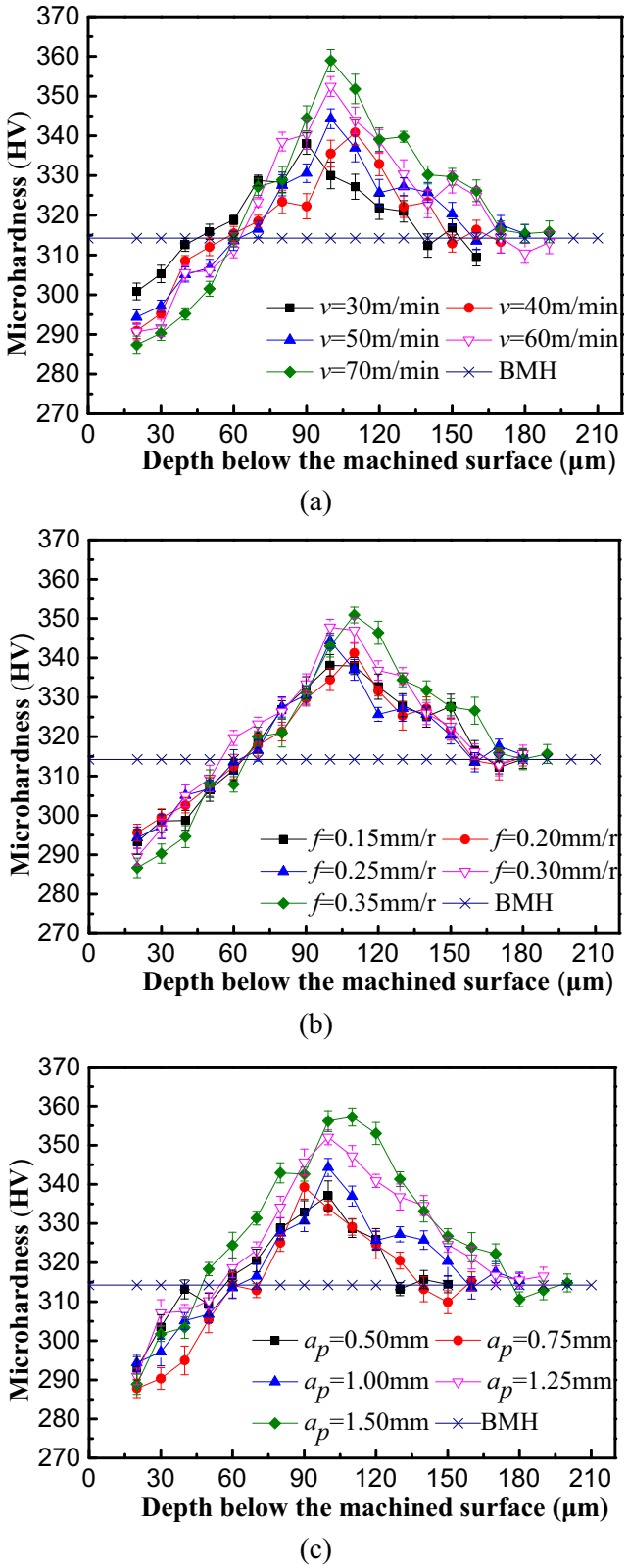

Fig. 4 The microhardness beneath the machined surface layer after roughing. **a** $f = 0.25$ mm/r, $a_p = 1$ mm. **b** $v = 50$ m/min, $a_p = 1$ mm. **c** $v = 50$ m/min, $f = 0.25$ mm/r

machined surface layer were generally consistent with other

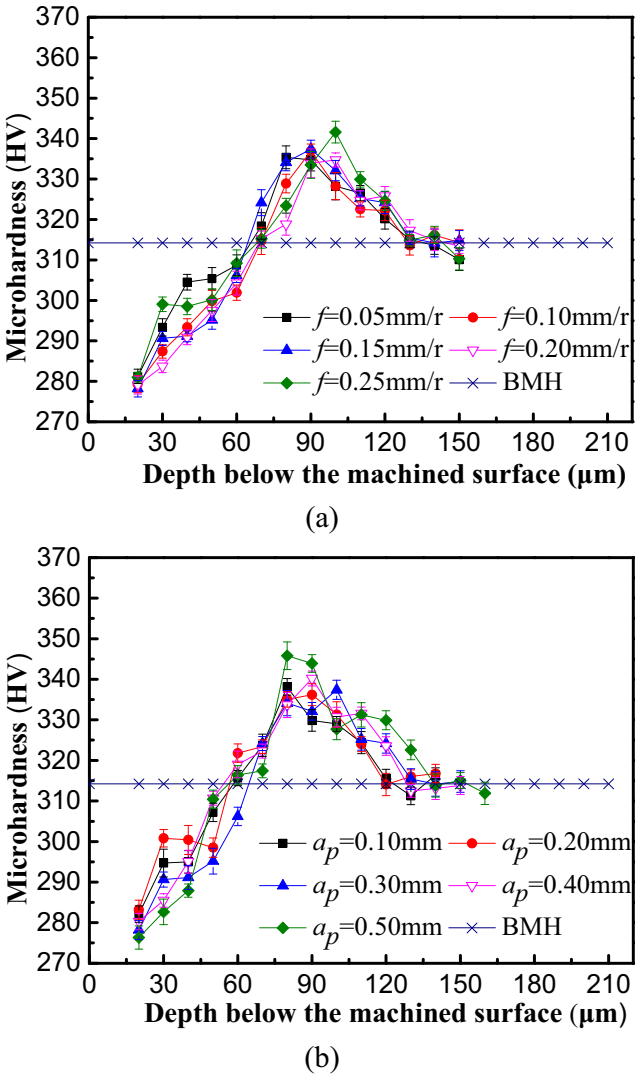

Fig. 5 The microhardness beneath the machined surface layer after semi-finishing. **a** $v = 80$ m/min, $a_p = 0.3$ mm. **b** $v = 80$ m/min, $f = 0.15$ mm/r

cutting process at the depths of cut of 0.3, 0.4, and 0.5 mm after the semi-finishing. In addition, the maximum microhardness value increased obviously with the increase of the depth of cut.

In high-speed cutting process, the material withstood high cutting force, cutting temperature, extrusion, friction, etc. [23], resulting in the change of material properties beneath the machined surface within a certain depth. When the depth was less than 60 μm beneath the machined surface, the microhardness was lower than the bulk microhardness of the material. Mainly because the influence of high cutting temperature on the machined surface layer was dominant when cutting, compared to the cutting force at the same depth, the closer the high cutting temperature was to the machined surface, the more obvious the dominant role was. At the same time, due to the poor thermal conductivity of titanium alloy, the surface layer softened by high cutting temperature decreased gradually with the

increase of depth, and the influence of cutting force on the surface layer gradually took the dominant role. Therefore, the microhardness of machined surface layer reached the maximum at a certain depth. Finally, as the depth continued to increase, the microhardness of machined surface layer affected by cutting force gradually weakened and eventually tended to the bulk microhardness (BMH) of 314.23 MPa.

It could be seen from the Fig. 4a–c that, as the roughing parameters increased, the microhardness decreased at 20 μm below the machined surface. At the same time, the maximum microhardness of the machined surface layer increased and the depth of hardening increased. Mainly because the increase of cutting parameters led to the increase of cutting temperature and cutting force [9]. In particular, Fig. 5a, b, due to the higher cutting speed in the semi-finishing, the cutting temperature was higher, which led to more severe softening near the machined surface layer. The microhardness was obviously lower than the microhardness in roughing at the same depth. At the same time, depth of cut was smaller in semi-finishing, so cutting force was relatively smaller; its effect on microhardness was relatively smaller; and the affected depth was also smaller. When the depth of cut was 0.1 mm in semi-finishing, although it was less than the hardening depth of roughing, due to the machined surface layer affected by the cutting temperature, the layer was softened near the machined surface in the semi-finishing cutting process. Especially in the range of 100–160 μm beneath the machined layer of roughing (the range of 0–60 μm beneath the machined layer of semi-finishing), the microhardness was lower than the bulk microhardness of the material after semi-finishing; therefore, it could be seen that the semi-finishing weakened the impact of roughing on the work hardening of machined surface layer.

3.2 Surface roughness and surface topography

In the single-step cutting process, compared to the cutting speed and the depth of cut, the effect of feed on the surface roughness was relatively larger [9]. However, it could be seen from Fig. 6a, b that as the cutting speed and feed increased, the surface roughness decreased firstly and then increased after finishing. However, it could be seen from Fig. 6c that, after finishing, the surface roughness was on the rise with the increase of roughing depth of cut. From Fig. 7a, b, it could be found that, compared to the effect of change of roughing cutting parameters on finishing surface roughness, the effect of semi-finishing was significantly reduced, which could be related to the microhardness at 0.1 mm below the machined surface during finishing cutting process.

Through the analysis, it was found that, due to the change of cutting speed, feed, and depth of cut in roughing cutting process, the surface roughness after finish machining varied from 0.378 to 0.485 μm, from 0.378 to 0.488 μm, and from 0.304 to 0.536 μm, respectively. At the same time, due to the change of feed and depth of cut in semi-finishing, the surface roughness after finishing machining varied from 0.282 to 0.357 μm and 0.282 to 0.367 μm, respectively. It could be seen that, compared to the effect of the change of roughing cutting parameters on finishing surface roughness, the effect of semi-finishing was smaller, and the variation range of surface roughness value was relatively smaller.

In the cutting process, affected by the cutting parameters, tool angle, and other aspects, the machined surface presents a certain degree of the convex peaks and concave valleys. In the ideal state, the concave valley is the path taken by the tool in the cutting direction. However, for the 3D surface topography

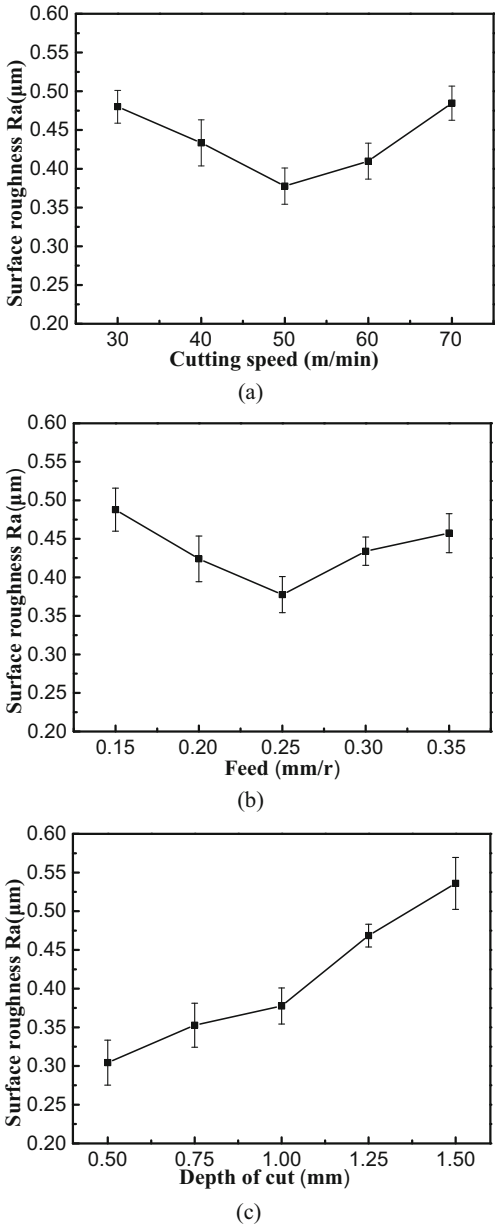

Fig. 6 The effect of change of roughing cutting parameters on finishing surface roughness. **a** $f = 0.25$ mm/r, $a_p = 1$ mm. **b** $v = 50$ m/min, $a_p = 1$ mm. **c** $v = 50$ m/min, $f = 0.25$ mm/r

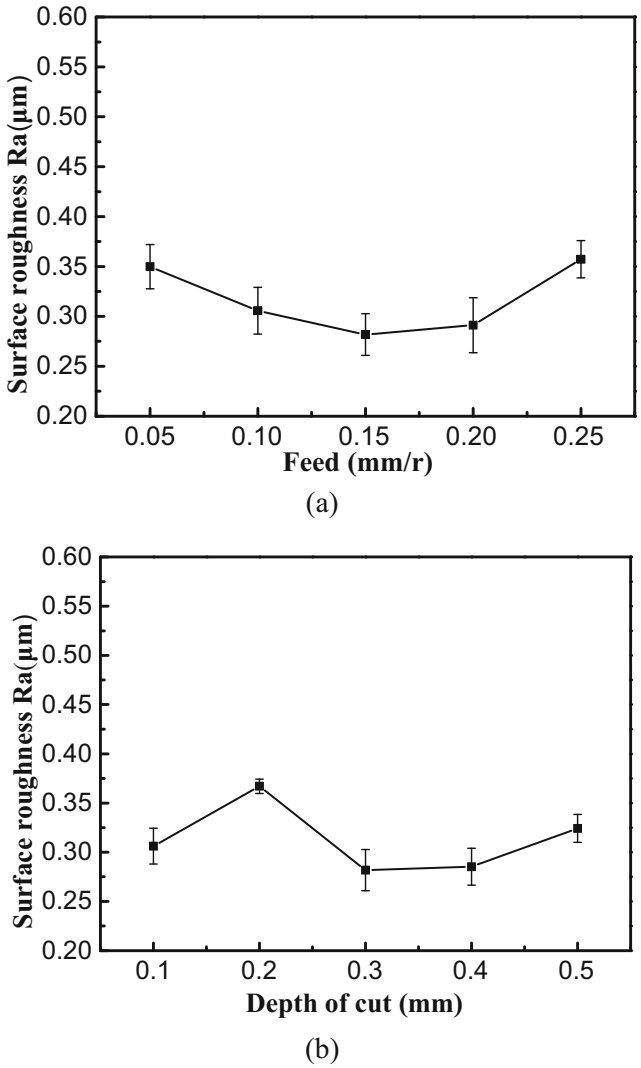

Fig. 7 The effect of change of semi-finishing cutting parameters on finishing surface roughness. **a** $v = 80$ m/min, $a_p = 0.3$ mm. **b** $v = 80$ m/min, $f = 0.15$ mm/r

of turning, it was mainly affected by the radius and feed, showing a certain peak-valley characteristics along the feed direction [22]. As can be seen from Figs. 8 and 9, the finishing surface topography was presented. From Fig. 8a–c, it could be seen that the change of roughing cutting speed had the most effect on the finishing surface topography and the depth of cut was the smallest. Compared to Fig. 8a–c, it could be seen from Fig. 9a, b that the surface topography of the three-step machining was significantly better than that of the two-step. From Fig. 8a–c, it could be found that the surface morphology of the two-step machining was greatly influenced by the change of roughing cutting parameters, and the relative height between the convex peak and the concave valley was larger. After two-step machining, it showed also the performance of the larger surface roughness values and the larger variation range of surface roughness. And the spacing between adjacent two convex peaks became larger and more uneven.

Through Figs. 6, 7, 8, and 9, it could be seen from the analysis and observation of finishing surface roughness and finishing surface topography that, compared to the three-step machining, when using two-step machining, the variation range the surface roughness values and surface topography was larger with the change of roughing cutting parameters. The main reason was that the machined surface layer was affected by the roughing or semi-finishing in the previous step, especially the work hardening and softening.

Compared to the change of the semi-finishing cutting parameters, roughing cutting parameters had greater influence on the microhardness of the machined surface layer, and the microhardness was higher. The microhardness under the surface of 100 μm, affected by the change of cutting parameters, had a significant difference. In particular, it could be seen from Fig. 4, as the depth of cut increases, the microhardness increases significantly at the surface of 100 μm, compared to the cutting speed and feed rate after rough machining. Although the same cutting conditions were used in finishing, due to the different microhardness affected by the previous

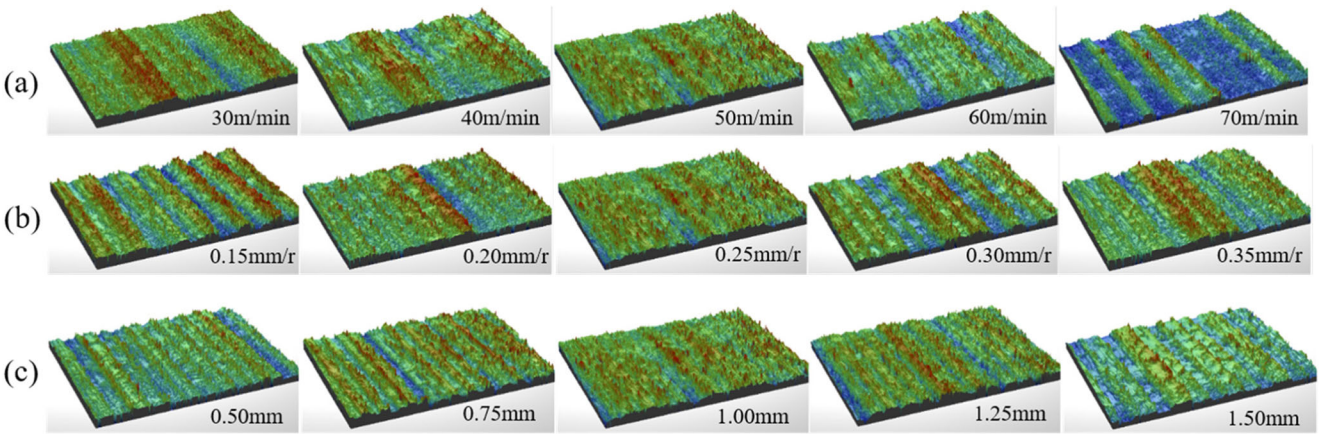

Fig. 8 The effect of change of roughing cutting parameters on finishing surface topography. **a** $f = 0.25$ mm/r, $a_p = 1$ mm. **b** $v = 50$ m/min, $a_p = 1$ mm. **c** $v = 50$ m/min, $f = 0.25$ mm/r

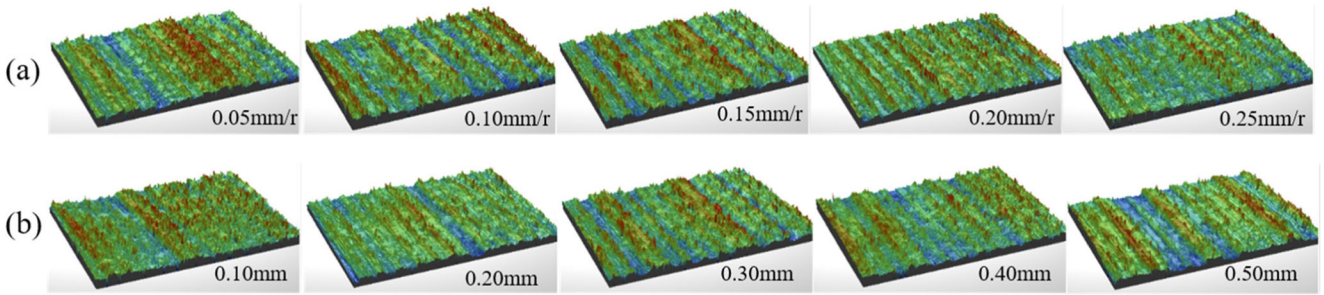

Fig. 9 The effect of change of semi-finishing cutting parameters on finishing surface topography. **a** $v = 80$ m/min, $a_p = 0.3$ mm. **b** $v = 80$ m/min, $f = 0.15$ mm/r

steps, cutting force and cutting temperature were also different. Because the greater the microhardness of the machined surface layer, the larger the cutting force and the higher the cutting temperature during the cutting process. The increase of the temperature in the area where tool, chip, and material contact with each other resulted in the increase of the material plasticity. The cutting force increased, and then the extrusion and friction between the cutting edge and the machined surface led to the plastic deformation of the machined surface so that the residual area was squeezed or uplifted intensely; eventually, surface roughness value became larger, and the surface topography became worse, as shown in Figs. 6 and 8.

At the same time, it was affected by the cutting process of the previous steps; especially, the cutting force, high cutting temperature, extrusion and friction, the work hardening ,and softening on the machined surface layer were relatively uneven after roughing, resulting in the uneven distribution of microhardness. Then, it further influenced finishing surface roughness and surface topography. At the same time, the uneven distribution of microhardness in machined surface layer after the previous steps, resulting in slight cutting vibration during finishing cutting processing, could also cause surface roughness to change.

3.3 Subsurface microstructure

In the cutting process, due to the influence of cutting force, high cutting temperature, extrusion, and friction, the material of machined surface layer within a certain depth is severely plastic deformed, which leads to the difference in material property between machined surface layer and the substrate Therefore, the grains are distorted, stretched, and fibrillated, causing the reduction of wear resistance, corrosion resistance, and fatigue life.

The results of finishing subsurface microstructure were presented in Figs. 10 and 11. It can be seen from Figs. 10 and 11 that all cutting directions were from right to left. It could be seen from Figs. 10 and 11 that, compared to the three-step machining, the depth of the disturbed layer or PDL after two-step machining was generally larger. The reason was that the microhardness of machined surface layer affected by roughing cutting process was higher, and the finishing cutting force was larger under the same cutting conditions, resulting in the greater impact on the subsurface microstructure.

It could be found from Fig. 10a, as the roughing cutting speed increased, the grains near the machined surface were more and more seriously distorted and stretched along the cutting direction, and deflection angle of grains was smaller. Even when the roughing cutting speed was 70 m/min, the grains were approximately parallel to the surface (P1 in the figure). Compared to Fig. 10a–c, it could be seen from Fig. 11a, b that the grains were generally severely distorted and stretched along the cutting direction after three-step machining. This was because, as the roughing cutting speed increased, the microhardness affected by the previous steps became larger beneath the machined surface layer after roughing. So the temperature was higher during finishing cutting process, the material was more easily softened by high cutting temperature and the plasticity became larger. Therefore, the intense plastic deformation caused the subsurface grains to be seriously distorted and stretched along the cutting direction, especially the grains near the machined surface. However, semi-finishing speed was higher, the heated material near the machined surface was more severely softened, and the increase of plasticity caused the grains to be more severely distorted and stretched during finishing.

Uneven surface morphology will affect the surface friction and wear, while the unevenly distorted and stretched grains after finishing will lead to uneven microhardness near the machined surface, which not only affect the initial friction and wear of the material on machined surface but also affect the material contact fatigue, reducing fatigue life. From Fig. 10b, it could be found that it was affected by the change of feed rate of the previous steps, and the deflection angle of grains near the machined surface along the cutting direction was obviously inhomogeneous. In some areas, the grain and the surface were nearly parallel (P1 in the figure), and in another areas, it maybe have a certain angle with the surface (P2 in the figure). At the same time, the PDL depth increased slightly, but not obviously. However, it could be seen from Fig. 11a that the PDL depth was relatively more homogeneous

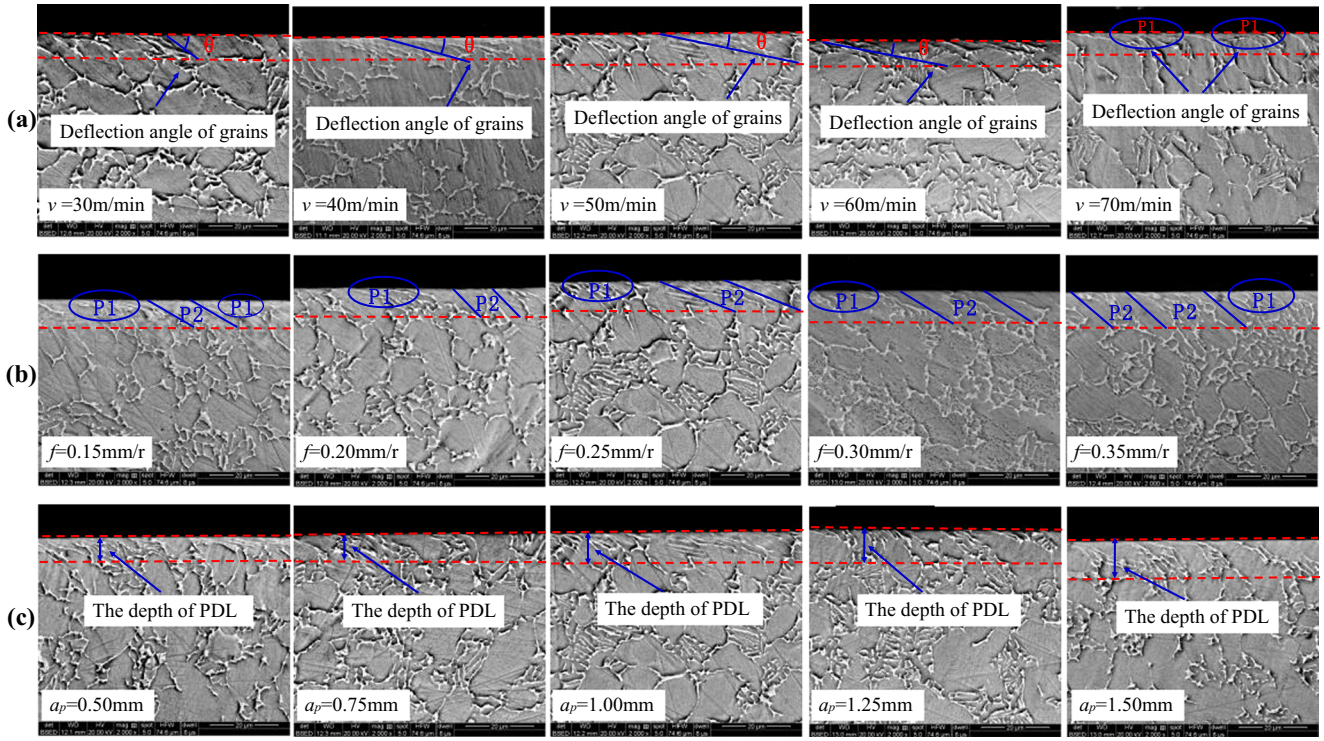

Fig. 10 The effect of change of roughing cutting parameters on the finishing subsurface microstructure. **a** $f = 0.25$ mm/r, $a_p = 1$ mm. **b** $v = 50$ m/min, $a_p = 1$ mm. **c** $v = 50$ m/min, $f = 0.25$ mm/r

and its depth was relatively smaller. The main reason was that, compared to semi-finishing, roughing depth of cut and feed was larger during the cutting process of the previous steps. And the distribution of work hardening and softening affected by the cutting force, high cutting temperature, extrusion, and friction was inhomogeneous beneath the machined surface layer after roughing, which resulted in uneven cutting force in finishing, and the cutting process was not stable. Eventually, deflection angle of grains was obviously different in different regions, and even the affected depth beneath the machined surface was different. At the same time, the finishing cutting vibration resulted from the uneven distribution of the microhardness also made the PDL depth uneven. However, because the semi-finishing weakened the impact of roughing on the work hardening of machined surface layer, subsurface microstructure is better.

It could be found from Fig. 10c that the affected depth increased obviously with the increase of the roughing depth of cut. However, it was also affected by the change of the depth of cut of the previous steps, and it could be found from

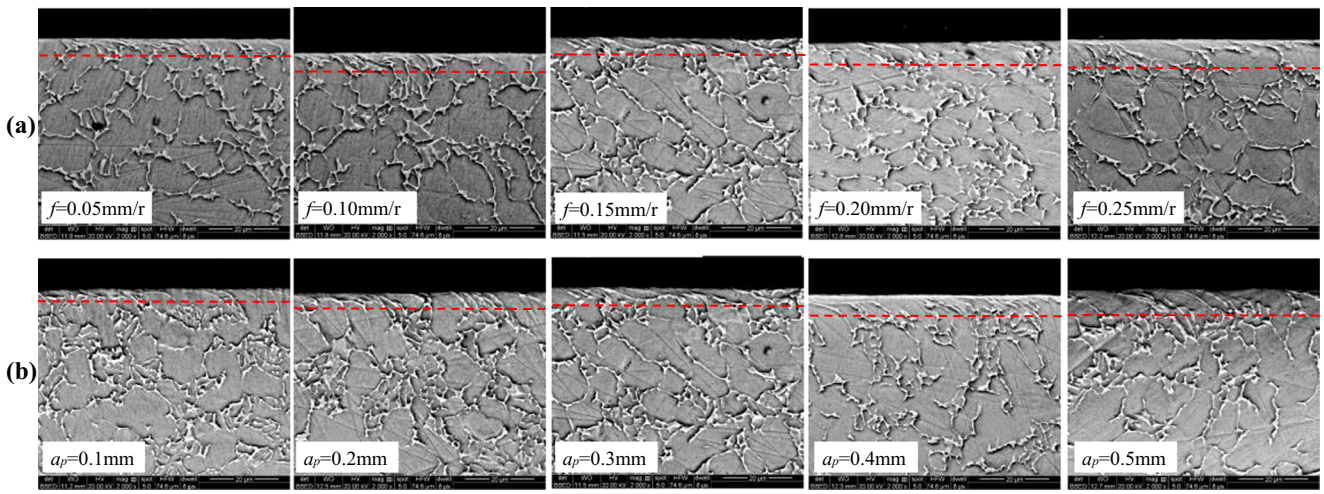

Fig. 11 The effect of change of semi-finishing cutting parameters on the finishing subsurface microstructure. **a** $v = 80$ m/min, $a_p = 0.3$ mm. **b** $v = 80$ m/min, $f = 0.15$ mm/r

Fig. 11b that the affected depth was relatively smaller. The reason was that, as the roughing depth of cut increased, the depth of work-hardened surface layer increased after roughing. Therefore, the cutting force increased during finishing, and then the affected depth of the subsurface microstructure would also increase. Although the three-step machining also included roughing, and the machined surface layer was work-hardened, there was a semi-finishing before finishing. Especially when the semi-finishing depth of cut exceeded the work-hardened depth affected by roughing, semi-finishing further weakened the effect of work hardening on the machined surface layer. Therefore, the effect of work hardening on subsurface microstructure decreased after finishing. Finally, it could be seen from Fig. 11b that, in order to reduce the effect on subsurface microstructure after finishing, the semi-finishing depth of cut should try not to exceed 0.3 mm.

4 Conclusion

Through the multi-step turning operations for the titanium alloy Ti-6Al-4V, the effect of work hardening and softening generated by the previous steps on finishing surface quality was studied, especially form the point of view of the surface roughness, surface topography, and subsurface microstructure. The conclusions are drawn as follows:

1. Compared to the microhardness of the machined surface layer after roughing, it was obviously smaller after semi-finishing at the same depth, and the affected depth was smaller. However, the softened depth affected by the high cutting temperature was bigger. At first, the material near the machined surface was severely softened. As the depth increased, the material affected by cutting force was gradually hardened. When reaching a certain depth, the cutting force effect was weakened, and the material microhardness decreased and finally approached the bulk microhardness.
2. In the two-step machining process, with the increase of roughing cutting speed and the feed, finishing surface roughness firstly decreased and then increased. The surface roughness value was the smallest at the cutting speed of 50 m/min or feed of 0.25 mm/r, respectively. However, the surface roughness value increased with the increase of roughing depth of cut. Compared to the two-step machining, the surface roughness value was not only smaller but varies more slightly with the parameters after three-step machining.
3. The change of roughing cutting speed had the greatest influence on the finishing surface topography and the depth of cut was smallest. The surface topography of the two-step machining was greatly influenced by the change of roughing cutting parameters, and the relative height between the convex peak and the concave valley was larger than three-step machining. And the spacing between adjacent two convex peaks became larger and more uneven.
4. In the two-step machining, as the roughing cutting speed increased, the grains near the machined surface were more seriously stretched and distorted after finishing. Even when machining at the cutting speed of 70 m/min, the affected grains were approximately parallel to the machined surface. Moreover, affected by roughing feed, the deflection angle of grains near the machined surface along the cutting direction was obviously inhomogeneous. However, with the increase of the roughing depth of cut, the affected depth increased obviously. Compared to the two-step machining, the disturbed layer depth or PDL depth after three-step machining was obviously reduced. At the same time, the deflection angle of grains near the machined surface along the cutting direction was relatively more homogeneous, but the grain near the machined surface was severely distorted and stretched.

Funding information The study was financially supported by the National Natural Science Foundation of China (51605260) and the Key Research and Development Program of Shandong Province - Public Welfare Special (2017GGX30144, 2018GGX103043).

References

1. Zhang CJ (1986) Titanium alloy machining technology. Northwestern Polytechnical University Press, Xi'an
2. Yang FR, Dong S (1988) Metal cutting principle. "Machinery Industry Press, Beijing
3. Zhou ZH, Yu QX (1993) Metal cutting principle. Science and Technology Press, Shanghai
4. Benardos PG, Vosniakos GC (2003) Predicting surface roughness in machining: a review. Int J Mach Tools Manuf 43(8):833–844
5. Yao CF, Wu DX, Ma LF, Tan L, Zhou Z, Zhang JY (2016) Surface integrity evolution and fatigue evaluation after milling mode, shot-peening and polishing mode for TB6 titanium alloy. Appl Surf Sci 387:1257–1264
6. Liu GL, Huang CZ, Zou B, Wang XY, Liu ZQ (2016) Surface integrity and fatigue performance of 17-4PH stainless steel after cutting operations. Surf Coat Technol 307:182–189
7. Hou CY, Chen ZT, Zhou ZT (2015) Influence of cutting speed and tool wear on the surface integrity of the titanium alloy Ti-1023 during milling. Int J Adv Manuf Technol 78(5–8):1113–1126
8. Liang XL, Liu ZQ (2017) Experimental investigations on effects of tool flank wear on surface integrity during orthogonal dry cutting of Ti-6Al-4V. Int J Adv Manuf Technol 93(5–8):1617–1626
9. Abboud E, Attia H, Shi B, Damir A, Thomson V, Mebrahtu Y (2016) Residual stresses and surface integrity of Ti-alloys during finish turning-guidelines for compressive residual stresses. Procedia CIRP 45:55–58

10. Ren XP, Liu ZQ (2016) Influence of cutting parameters on work hardening behavior of surface layer during turning superalloy Inconel 718. Int J Adv Manuf Technol 86(5–8):2319–2327
11. Choi Y (2017) Influence of rake angle on surface integrity and fatigue performance of machined surfaces. Int J Fatigue 94:81–88
12. Rotella G, Dillon OW Jr, Umbrello D, Settineri L, Jawahir IS (2014) The effects of cooling conditions on surface integrity in machining of Ti6Al4V alloy. Int J Adv Manuf Technol 71(1–4): 47–55
13. Matsumoto Y, Barash MM, Liu CR (1986) Effects of hardness on the surface integrity of AISI 4340 steel. Trans ASME, J Eng Ind 108:169–175
14. Dehmani H, Salvatore F, Hamdi H (2013) Numerical study of residual stress induced by multi-steps orthogonal cutting. Procedia CIRP 8:299–304
15. Dehmani H, Salvatore F, Hamdi H (2013) Multistep hybrid approach applied to material removal operation using cutting tool. 21st French Congress of Mechanics, August 26–30, Bordeaux, France (FR)
16. Li JL, Jing LL, Chen M (2009) An FEM study on residual stresses induced by high-speed end-milling of hardened steel SKD11. J Mater Process Technol 209(9):4515–4520
17. Liu CR, Guo YB (2000) Finite element analysis of the effect of sequential cuts and tool-chip friction on residual stresses in a machined layer. Int J Mech Sci 42(6):1069–1086
18. Sasahara H, Obikawa T, Shirakashi T (1996) FEM analysis of cutting sequence effect on mechanical characteristics in machined layer. J Mater Process Technol 62(4):448–453
19. Che-Haron CH, Jawaid A (2005) The effect of machining on surface integrity of titanium alloy Ti–6%Al–4%V. J Mater Process Technol 166(2):188–192
20. Ginting A, Nouari M (2009) Surface integrity of dry machined titanium alloys. Int J Mach Tools Manuf 49(3):325–332
21. Deng XY (2012) The simulation research on the machining mechanism during high speed cutting of titanium alloys. M.S. Dissertation, Shenyang Ligong University
22. Velásquez JDP, Tidu A, Bolle B, Chevrier P, Fundenberger JJ (2010) Sub-surface and surface analysis of high speed machined Ti–6Al–4V alloy. Mater Sci Eng A 527(10–11):2572–2578
23. Chen T (2015) Theory and method of surface integrity in machining. Science Press, Beijing